B041 Rock Physics Diagnostic in Sand/Shale Sequence

Jack Dvorkin[1], Matthew B. Carr[2], and Tim Berge[3]

1) Stanford University 2)Rock Solid Images, and 3)Forest Oil
397 Panama Mall, Mitchell 315
Geophysics Department
Stanford University
Stanford, CA 94305-2215

Abstract

The rock physics diagnostic is a procedure of establishing a rational effective-medium-based transform between the elastic and bulk properties of the sediment. A typical example of such transform is a porosity-impedance relation. Often, the rock physics diagnostic allows the geoscientist to relate the elastic properties not only to the sediment bulk properties but also to its conditions, such as effective pressure and saturation. The main purpose of the rock physics diagnostic is to derive reservoir properties and conditions from seismic data by, e.g., directly applying a rock physics transform to an impedance volume. Another common application of a rock physics transform is in creating synthetic seismograms by perturbing bulk rock properties and determining the corresponding perturbations of the elastic properties. Pore fluid (saturation) perturbation is commonly used to predict the seismic response of a reservoir under varying saturation conditions. Rational rock physics transforms allow the geoscientist to go further, and consistently predict the seismic response of geobodies with varying porosity and mineralogy. Presented here is the rock physics diagnostic performed for a thick sand/shale sequence from offshore South Africa. The result of this diagnostic is a physically consistent model that relates the acoustic impedance to the total porosity and clay content. The model can be used to track porosity, lithology, and saturation from impedance inversion.

Data Display, Crossplots, and Their Physical Meaning

In Figure 1 we display well log curves in a vertical well for depth ranging from 1.7 to 3.4 km. The gas reservoir is located at about 3.2 km and is marked by low gamma ray (GR) values, high resistivity values, low bulk density values, relatively high porosity values, and relatively low P-wave impedance values. The entire sequence exhibits distinctive compaction that is expressed in resistivity, bulk density and the impedance monotonically increasing with depth, and porosity monotonically decreasing with depth.

The impedance curve essentially mirrors the total porosity curve and also the neutron porosity curve, which should result in distinctive impedance-porosity trends. Figure 2 shows that such trends do exist. However, theses trends cannot be directly used in porosity prediction because of a significant scatter of the data points around the mean trends and the resulting non-uniqueness. The observed non-uniqueness is a result of lithological variations. The effect of clay content on the impedance can be

observed in Figure 3. This figure duplicates Figure 2 except the data are segregated by GR cutoff values exhibiting only low-GR (GR<15 GAPI) and high-GR (GR>125 GAPI) data points.

Both very clean and very shaley rocks exhibit sharp low-scatter impedance-porosity trends. The more clay that is present in the rock the softer it is at given porosity. This behavior is well known and consistent with the effects observed by Han (1986). The consolidated sandstone samples from Han (1986) exhibited porosity ranging from 0% to 30% and clay content ranging from 0% to nearly 50%. Data for selected samples from this database are shown in Figure 2. They form an upper bound for the impedance data points in the interval under examination.
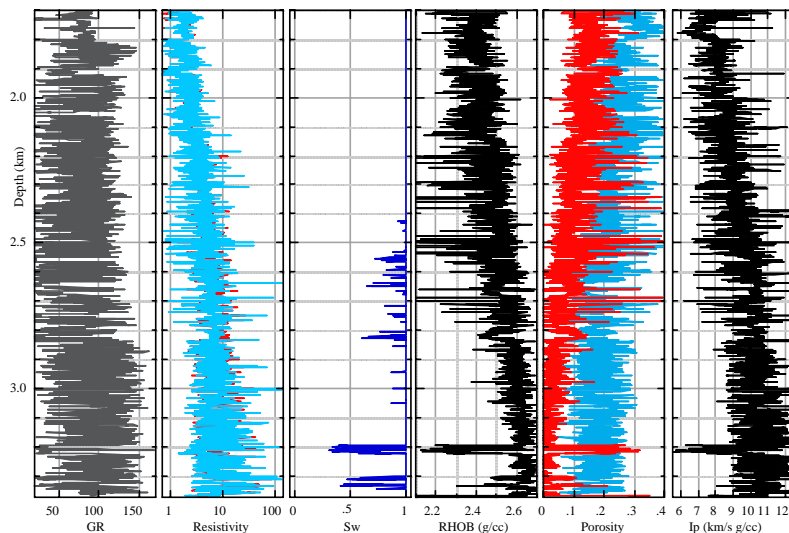
Figure 1. Well log curves. The porosity frame shows the density-derived total porosity (red) as well as neutron porosity (blue). The main gas reservoir is at about 3.2 km.

| Figure 2. Impedance versus total (density-derived) porosity (left) and neutron porosity (right) for the interval shown in Figure 1. The large red symbols in the left-hand frame are for selected medium-clay-content sandstone samples from Han's (1986) data set. | Figure 3. Impedance versus total (density-derived) porosity (left) and neutron porosity (right) for the interval shown in Figure 1. The red symbols are for low-GR cutoff (GR < 15); the green symbols are for high GR cutoff (GR > 125). |

Consider next the combined effect of porosity and lithology on the elasticity of the interval. Exhibited in the left side plot in Figure 4 is the P-wave impedance versus the total porosity, color-coded by GR values. Apparent in this plot are sharp low-scatter trends for constant-GR subsets. The higher the GR the more clay is present in the rock the smaller the impedance at a fixed porosity. The constant-GR trends can also be treated as compaction trends for fixed lithologies. The effect of compaction on porosity and impedance is also apparent in Figure 4, right, where the impedance-porosity cross plot is color-coded by depth. The dark-red data points that have high porosity and low impedance are from the gas-saturated pay zone at about 3.2 km.
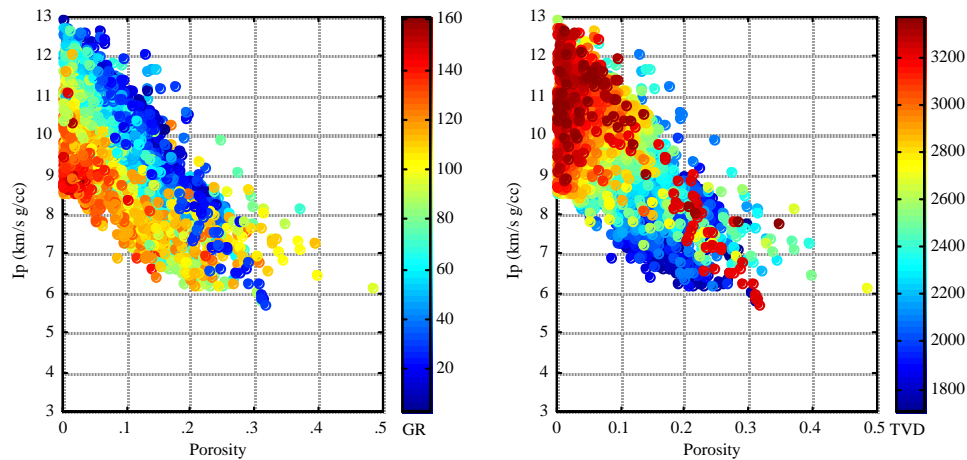
Figure 4. Impedance versus total (density-derived) porosity color-coded by GR (left) and by depth (right). The high-porosity dark red points in the right-hand frame are from gas-saturated sand interval.

The Reservoir and the Rock Physics Model

The reservoir interval is detailed in Figure 5, where shown are well log curves, the same as in Figure 1. The gas zone is marked by two low-GR sections, separated and bounded by high-GR shale zones. Crossover of the density-derived porosity and neutron porosity curves, as well as the test data, indicate gas-bearing sandstones.

We perform theoretical fluid substitution in the interval to calculate the impedance in 100% water saturated rock, according to the Vp-only method of Mavko et al. (1995). The resulting impedance curve (blue in the impedance frame of Figure 5) lies, as expected, to the right of the measured (red) impedance curve. Fluid substitution allows us to directly compare the reservoir to other rocks that are fully water saturated.

To diagnose the reservoir we compare it to the well-studied Han's (1986) data base (Figure 6). The clean sands in the reservoir exhibit a sharp almost liner impedance-porosity trend. The subset of Han's data with clay content between 5 and 20% of clay precisely mimics the clean-sand trend in the pay zone. The subset of Han's data with clay content above 25% continues the shale data from the pay interval into a higher-porosity range. Together, Han's shale and the shale from the well form an impedance-porosity trend that lies below the clean-sand trend. This elastic-analogy diagnostic not only determines trends in the data but also serves as QC for the well

log measurements and derived bulk and elastic properties. The final step is to find an appropriate rock physics model that mimics the well data and can be used for porosity and lithology mapping from seismic. Such a model -- the modified upper Hashin-Shtrikman model (yet unpublished) -- has been developed for describing well-consolidate sandstones and carbonates. The model lines are superimposed on the pay zone well log data in Figure 6. This model accurately describes the data and thus can be used as a rational rock physics transform to map porosity in the reservoir under examination.

Discussion and Conclusion

By applying the rock physics diagnostic to well log data we find a rational model that relates the elastic properties to porosity and clay content. The model can be used to map porosity from impedance inversion. The impedance depends on at least three variables that are porosity, clay content, and pore fluid. The apparent non-uniqueness in porosity mapping can be resolved if shear-wave data are used which may come from elastic impedance inversion.
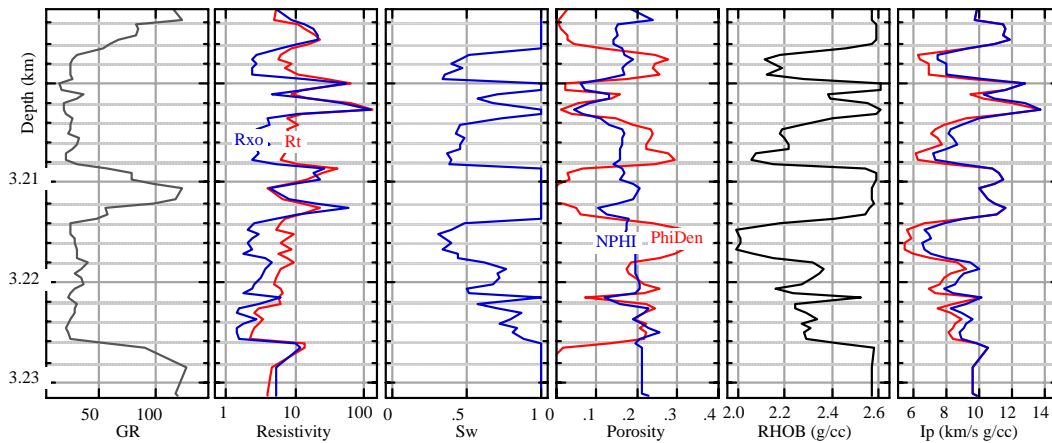
Figure 5. Well log curves in the pay zone. The impedance curve shows the measured impedance (red) and also the impedance theoretically computed for the same rock at 100% water saturation (blue).
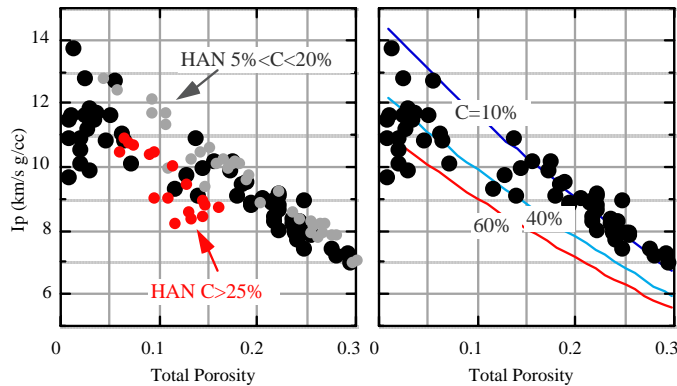
Figure 6. Impedance versus total (density-derived) porosity with Han's data superimposed (left) and model lines superimposed (right). The clay content ("C") in the data and in the model is shown in the frames.

Acknowledgment

References

Mavko, G.., Chan, C., and Mukerji, T., 1995, Fluid substitution: Estimating changes in Vp without knowing Vs, Geophysics, 60, 1750-1755.

Han, D.H., 1986, Effects of porosity and clay content on acoustic properties of sandstones and unconsolidated sediments, Ph.D. dissertation, Stanford University.